Modeling and Numerical Simulation of an Immobilized Enzyme Conductometric Urea Biosensor

Sid-Ali Kouras
LEA Laboratory, Electronic Department, University of Batna 2 "Mostefa Ben Boulaïd", Batna, Algeria | Electric Department, University of Ouargla, Ouargla, Algeria
sid-ali.kouras@univ-batna2.dz (corresponding author)

Ramdane Mahamdi
LEA Laboratory, Electronic Department, University of Batna 2 "Mostefa Ben Boulaïd", Batna, Algeria
r.mahamdi@univ-batna2.dz

Naima Touafek
Higher National School of Biotechnology "Toufik khaznadar", Ville University Ali Mendjeli, Algeria
ntouafek@yahoo.fr

Fouad Kerrour
Laboratory of Renewable Energy Devices Modeling and Nanoscale MODERNA, Department of Electronics, University of Constantine 1, Constantine, Algeria
f_kerrour@yahoo.fr

Received: 11 February 2025 | Revised: 7 March 2025 | Accepted: 19 March 2025

 DOI: https://doi.org/10.48084/etasr.10529

ABSTRACT

In this study, a mathematical model for predicting the response of a conductometric urea biosensor was developed and numerically simulated. The biosensor features a planar interdigitated electrode array with immobilized urease. The enzymatic hydrolysis of urea generates ionic products, such as ammonium (NH_4^+) and bicarbonate (HCO_3-) ions, altering the solution's electrical conductivity. To optimize the biosensor performance, key physicochemical processes were analyzed through numerical modeling and validated against experimental data, showing strong agreement. Simulations under varying conditions supported the experimental design, improved the analytical performance, and reduced the development costs. While previous studies have explored conductometric urea biosensors, few have addressed optimizations through numerical modeling. This study addresses this gap by examining the effects of temperature, pH, enzyme layer thickness, and CO_2 concentration using the COMSOL Multiphysics software. The model accurately predicted conductivity variations across different urea concentrations, with optimal responses being observed at 37 °C, 5% CO_2, pH 7.4, and an enzymatic zone length of 500 µm. These results offer valuable insights for enhancing the design and application of conductometric urea biosensors in biomedical and environmental fields.

Keywords-conductometry; urea; urease; modeling; biosensor; immobilized enzyme

I. INTRODUCTION

Electrical conductivity measures the ability of a solution to conduct a power flow that depends on the concentration and mobility of the ions present in the solution (σ) [1], also defined as the ability of a solution to carry an electric charge. It is usually expressed in Siemens per meter (S/m) or micro-siemens per centimeter (µS/cm). Conductometric sensors can be used to detect specific substances, such as urea in the case of urea-based biosensors. The variation in conductivity is then bonded to a specific enzymatic or chemical reaction [2]. Urea is an organic compound with the chemical formula $CO(NH_2)_2$, consisting of two amine groups (NH_2) bonded to a carbonyl group (C=O). It is a metabolic waste product produced in the liver during the urea cycle, which is intended to eliminate toxic ammonia from protein degradation [3]. Blood and urine urea concentrations are often measured to assess kidney function,

with high levels of blood urea (called uremia) indicating kidney failure or other health issues. [4]

The key element of the sensor is the urease enzyme, which is immobilized on the sensor surface. Urease catalyzes the decomposition of urea into ammonia (NH_3) and carbon dioxide (CO_2), producing ammonium (NH_4^+) and hydroxide (OH^-) ions in the presence of water, which alters the physicochemical properties of the solution, as shown in:

$$CO(NH_2)_2 \xrightarrow{urease} 2NH_4^+ + CO_2 + 2OH^- \quad (1)$$

These ions change the electrical conductivity of the solution, and the sensor detects these changes, which are directly proportional to the concentration of urea in the solution. Thus, by measuring these changes, the sensor can determine the concentration of urea in a sample [5, 6]. The conversion into a measurable signal is performed by a transducer. The signal can be of different types, depending on the principle used. In this case, the principle of conductimetry is utilized, where the sensor measures the change in the conductivity of the solution due to an increase in NH_4^+ and OH^- ions.

This paper has modeled the phenomena occurring near the surface of the electrodes of a conductometric biosensor. Within this region, electrolyte ions experience attraction and repulsion due to the excess charge on the electrode, forming a diffuse double layer, a nanometer-scale zone influenced by electrolyte concentration, potential difference, and enzymatic hydrolysis of urea. Notably, the assumption of local electroneutrality does not hold in this region [7, 8]. To account for both mass and charge transfer, the present work coupled diluted species transport with electrostatics [9]. The model adheres to fundamental electrochemical laws, linking thermodynamic and kinetic properties to experimental conditions and device performance:

- The Nernst equation describes the electrochemical potential as a function of species concentration in the reaction.
- The Butler-Volmer equation [10] relates current density to overpotential (the difference between the applied potential and the equilibrium potential); at high overpotentials, it simplifies to the Tafel equation.
- Faraday's law quantifies the relationship between substance conversion and electrical charge [11].
- The Cottrell equation models current density evolution over time in a diffusion-controlled process at a flat electrode.

This study proposes a numerical model implemented into COMSOL Multiphysics [12] for the modeling of the coupling charge transfer with mass transfer. The geometry of the transducer, composed of interdigitated microelectrodes on the surfaces of a urease enzyme layer, was taken into account. Careful consideration was given to the boundary and initial conditions. Biosensor parameters were derived from literature data, but for model validation, experimental data of urea detection were used. To optimize sensor performance, this study simulated responses across various urea concentrations and electrode geometries [13].

II. MODELING

To increase the conductivity of the electrolyte, supporting electrolytes are introduced in electroanalytical experiments. These substances do not interfere with the chemical reaction, ensuring that the solution resistance remains stable, and the electric field is negligible. As a result, a constant electrolyte potential is assumed, given by:

$$\phi_l = 0 \quad (2)$$

To describe the diffusion of chemical species, Fick's Second Law is employed, which at steady state simplifies to:

$$\nabla(D_i \nabla_{c_i}) = 0 \quad (3)$$

The model accounts for several species, including the acid-base reaction pairs NH_4^+/NH_3, the acid-base dissociation reactions of the H_2CO_3/HCO_3^- pair, the HCO_3^-/CO_3^{2-} pair, as well as the concentration of the urea analyte species. Some urea hydrolysis byproducts are ignored as they do not impact sensor behavior.

The rate of this reaction (mol/m^3) is given by a Michaelis–Menten rate law as:

$$R = \frac{C_{urea} V_{max}}{1 + K_m C_{urea}} \quad (4)$$

where V_{max} is the maximum enzymatic reaction rate, depending on the quantity of enzyme available, and the parameter K_M is the characteristic Michaelis-Menten coefficient. At high urea concentration, the rate becomes independent of the urea concentration and solely depends on the enzyme kinetics.

The concentrations [mol/m^3] of species in the electrolyte phase are time- and position-dependent, as described by:

$$\frac{\partial C_u}{\partial t} = D_u \frac{\partial^2 C_u}{\partial x^2} - R_u \quad (5)$$

$$\frac{\partial C_p^i}{\partial t} = D_p^i \frac{\partial^2 C_p^i}{\partial x^2} - R_p^i \quad (6)$$

where the subscript u denotes the urea, while the subscript p denotes the product of the reaction. C_u and C_p^i represent the concentrations of urea and the i^{th} product, respectively. D_u and D_p^i represent the corresponding diffusivities and are assumed to be independent of time and space. The terms R_u and R_p^i are reaction terms, representing the rate of disappearance of urea and the products, respectively.

The rate of urea consumption at $x = 0$ is assumed to follow Michaelis-Menten kinetics [14]:

$$R_u|_{x=0} = V_{max} \frac{C_u^s}{C_u^s + K_M} \quad (7)$$

where C_u^s is the urea concentration at the sensor surface. This expression is used when urea concentrations are relatively low [15].

To model the behavior of ions under the influence of concentration gradients, electric fields, and to describe the ionic flux C_u^s of an ionic species i, the Nernst-Planck equation is utilized, which is the sum of three main contributions:

$$J_i = -D_i \nabla c_i - \mu_i z_i F c_i \nabla \phi \quad (8)$$

where D_i [m^2/s] is the diffusion coefficient, μ_i [s·mol/kg] is the mobility, F [C/mol] is the Faraday constant, and ϕ [V] is the electric potential in the electrolyte phase.

The conservation of mass when there is no homogeneous reaction of ions in the solution, for both species, is:

$$\nabla \cdot J_i = 0 \quad (9)$$

For electric potential, Gauss's Law (Poisson's equation) applies:

$$\nabla \cdot (-\varepsilon \nabla \phi) = \rho \quad (10)$$

where ε is the permittivity [F/m] and ρ the charge density [C/m^3].

The electrical conductivity is calculated as:

$$\sigma = \sum_i |z_i| F \mu_i c_i \rho \quad (11)$$

where σ is the conductivity [$\mu S \cdot cm^{-1}$], z_i is the charge of the ion i, c_i [$mol \cdot cm^{-3}$] is the molar concentration of the i^{th} ionic species.

A. Initial Conditions

Initial conditions assume spatially uniform concentrations of all species. The urea concentration was initialized to the value of interest. The concentrations of all products were zero. The initial conditions are given as:

$$C_u = C_0 \quad (12)$$

$$C^i_{p_{surface}} = C^i_{p_{bulk}} \quad (13)$$

where C_0 is the concentration of urea in the bulk solution.

B. Boundary Conditions

At the sensor surface, the flux of substrate and products passing from one layer to another is assumed to be equal. The flux of urea and products away from the surface is given by:

$$D_u \left.\frac{\partial c_u}{\partial x}\right|_{x=0} = R_u|_{x=0} \quad (14)$$

$$D^i_p \left.\frac{\partial c^i_p}{\partial x}\right|_{x=0} = R^i_p|_{x=0} \quad (15)$$

At the bulk boundary, the concentration is uniform for each chemical species, equal to its bulk concentration. The urea concentration here is equivalent to that in the analyte mixture being measured [16]. The molar conductivity of the electrolyte at infinite dilution is given by Kohlrausch's law of independent ion migration. It states that the molar conductivity of an electrolyte at infinite dilution can be expressed as the sum of the individual contributions of cations and anions. At infinite dilution, the ions in an electrolyte solution are so far apart that they do not interact with each other. As a result, each ion contributes independently to the total molar conductivity. Kohlrausch's law is useful in determining the conductivity of electrolytes, and it is also used to calculate the dissociation constant of weak electrolytes.

III. FIELD MODEL

The sensor consists of interdigitated electrodes alternating positive and negative fingers, arranged in parallel on a plane. Each pair of fingers forms a region where the electric field is generated when a potential difference is applied between the electrodes. The simulation has enabled calculating the interelectrode conductance with the electric field equations for the geometry of a single pair of interdigitated electrode arrays. The electric field model solves the Laplace equation using collocation methods to match the mixed boundary conditions in the electrode plane [17]. Laplace's solution provides a complex admittance, encompassing both conductance and capacitance, of the electrode array. Key parameters influencing conductivity include interelectrode spacing, electrode width, and spatial period, which is the distance between the centerline of one electrode digit and the corresponding position on the next digit of the same electrode. The model accounts for the non-uniform properties of the bulk (urea solution) in the normal direction to the surface of the electrode array. The bulk conductivity has been determined from the overall ion concentration, as represented by (14).

IV. RESULTS AND DISCUSSION

The conductometric urea sensor model has been validated using reasonable estimates of parameters, such as the diffusivities of urea and its hydrolysis products, as well as the kinetics of the immobilized enzyme. The diffusivity of urea in aqueous solution has been set to 1.38×10^{-5} cm^2/s, with a single diffusion coefficient applied to the ionic hydrolysis products. Urea hydrolysis kinetics have been modeled using the Michaelis-Menten equation, considering the low urea concentrations in the experiments. The K_M of urease has been set to 4.0 mM, and V_{max} has been estimated based on the urease coverage on the sensor surface [18]. Since urease is immobilized only above the electrode array, the surface reaction rate V_{max} is estimated to be $3.6\text{x}10^{-10}$ $mol/cm^2 \cdot s$. A fluid velocity of 2.5 cm/s on the sensor substrate has been estimated. The conductance curve of the interdigitated electrode array has been calculated for each tested urea concentration, showing a more rapid increase in conductivity at low urea concentrations than the one observed experimentally. To refine the model, the initial conditions have been adjusted to account for CO_2, and model predictions have been compared with and without its influence.

The conductometric sensor model for different urea concentrations incorporates various parameters. The diffusion coefficient of the substrate in the diffusion layer (D^i_p) has been estimated between 1.40×10^{-8} and 2.23×10^{-8} cm^2/s. The diffusivity of urea (D_u) in the enzyme layer has been estimated between 9.50×10^{-7} and 4.12×10^{-7} cm^2/s. As for the products, the effective diffusion coefficient (D_{eff}) in the enzyme membrane has been estimated between 4.20×10^{-8} and 7.10×10^{-8} cm^2/s.

A. Static Study

The static study examines the sensor's behavior at equilibrium, where enzymatic reactions and ion diffusion have stabilized. This eliminates time dependence, simplifying complex differential equations into solvable algebraic equations. At equilibrium, the measured conductivity reflects the final concentrations of the ionic hydrolysis products, NH_4^+ and HCO_3^-, following complete urea hydrolysis.

Figures 1-3 display typical concentration profiles for urea, NH_4^+, and HCO_3^- within the unit cell. These ions are generated in the solution between the electrodes and the ground through the enzyme-catalyzed hydrolysis of urea. The reaction occurs at the anode in the center of the unit cell, altering the conductivity of the solution between the working electrodes used to measure the urea concentration. HCO_3^- is regenerated at the counter cathode electrodes located on the left and right sides of the cell. The diffusion of $HCO_3^-$and NH_4^+ between the interdigitated electrodes is the process through which multiple reactions are driven in opposite directions at two electrodes with a small geometric separation.

The concentrations of the products of the enzymatic reaction in steady state are concentrated at a maximum of 50 μm from the electrodes. These concentrations decrease or increase as they approach the surface of one electrode or the other. This difference is due to the stoichiometric coefficients.

Figures 2 and 3 illustrate the concentrations of NH_4^+ and HCO_3^-, along with a zoomed-in view of the corresponding electrode interface. The maximum and minimum concentrations are observed at the electrode surface and gradually vary within the volume, following the expected theoretical trends.

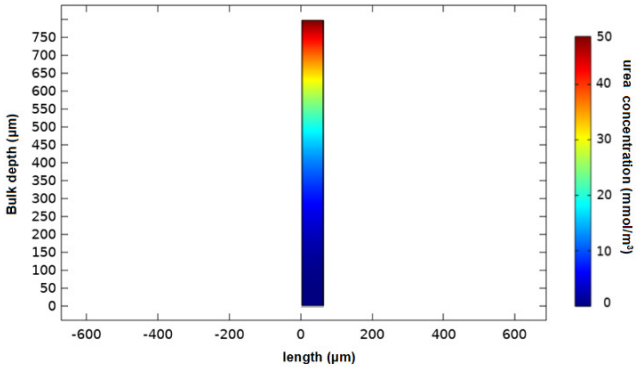

Fig. 1. Urea concentration for an external concentration of 1000 mol/m^3. Two-dimensional urea concentration profiles in the diffusion layer and enzyme membrane for general stationary studies.

To better visualize the progression of urea concentration, a one-dimensional concentration profile was extracted along a specific path in the two-dimensional field. This approach highlights subtle gradients and provides a clearer insight into concentration variations that are not easily discernible in full 2D plots, as portrayed in Figure 4.

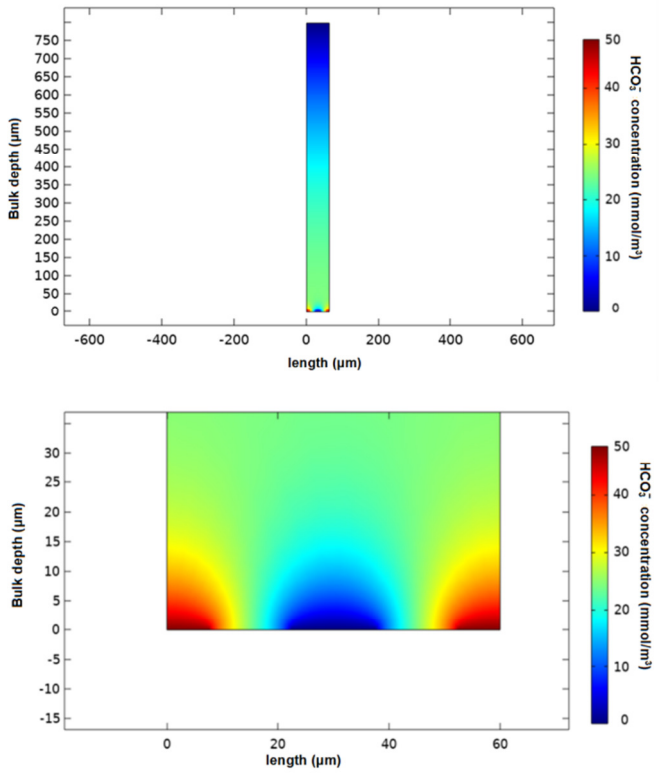

Fig. 2. Two-dimensional HCO_3^- concentration profiles for an external urea concentration of 50 mmol/m^3, in the bulk and the diffusion layer and enzyme membrane for general stationary studies.

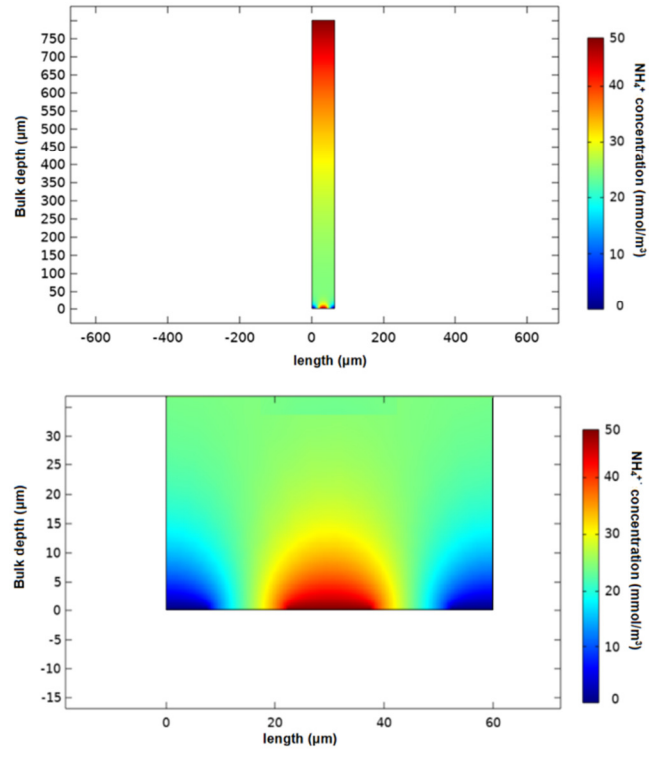

Fig. 3. Two-dimensional NH_4^+ concentration profiles for an external urea concentration of 50 mmol/m^3, in the bulk and the diffusion layer and enzyme membrane for general stationary studies.

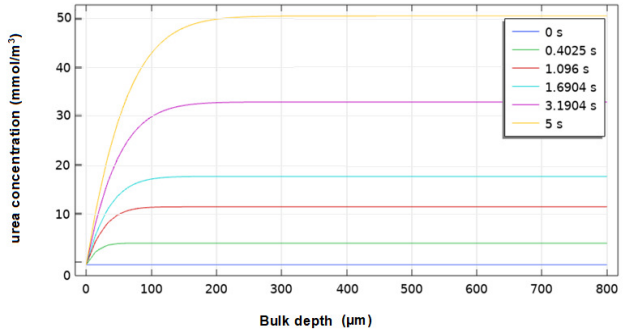

Fig. 4. One-dimensional urea concentration profile for an external urea concentration of 50 mmol/m^3, in the bulk and the diffusion layer and enzyme membrane at different time intervals.

As shown in Figure 4, the maximum concentration occurs consistently within the first 200 µm from the surface, emphasizing that the diffusion and reaction processes are most intense near the interface. This indicates that most of the urea transport and enzymatic activity are concentrated in this region. Furthermore, it is notable that the maximum concentration is reached within 5 seconds of the reaction initiation. After this initial period, the concentration stabilizes, indicating a rapid initial response followed by a slower, diffusion-driven transport of urea through the membrane.

B. Dynamic Study

Unlike the static study, the dynamic study enables the analysis of the kinetics of enzymatic reactions, ion diffusion, and the temporal response of the sensor to variations in external conditions, such as urea concentration, temperature, or pH. This dynamic approach provides critical insights into key performance parameters, including response time, stability, and reproducibility of the sensor. Understanding these characteristics is essential for real-time applications and for ensuring reliable operation in environments where conditions may fluctuate.

1) Model Validation

The model validation process is essential to assess the model's ability to predict the sensor's response under various conditions, including changes in urea concentration, temperature, pH, and other influencing factors. A strong agreement between the simulated and experimental results confirms that the mathematical assumptions and parameters employed accurately reflect the real behavior of the biosensor.

Figure 5 presents a comparison between the experimental results (triangular markers) [14] and theoretical simulations (solid lines) derived from the mathematical model developed for the conductometric urea biosensor using COMSOL Multiphysics simulations. It demonstrates a strong correlation between experimental data and theoretical simulations. Both the experimental points and the simulated curves exhibit a similar trend, characterized by a rapid initial increase in conductivity due to enzymatic activity, followed by a plateau as the reaction reaches equilibrium. This behavior reflects the production of HCO_3^- and NH_4^+ during urea hydrolysis, which alters the solution's conductivity. Minor discrepancies between the experimental data and the theoretical curves may result from experimental variations not accounted for in the model, such as temperature fluctuations or inconsistencies in enzyme immobilization. Overall, these results confirm the model's reliability in predicting the biosensor's response under varying conditions.

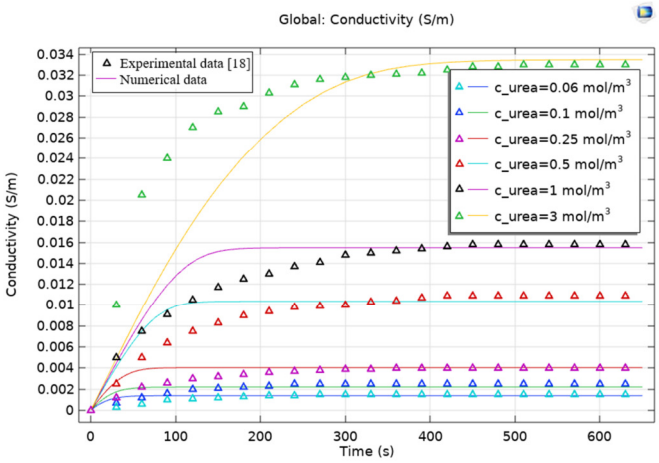

Fig. 5. The theoretical results and the experimental data [14] of the conductometric biosensor response for different concentrations of urea.

2) Calibration Curves

The numerical simulation of the previously described mathematical model was successfully implemented to calibrate the response of the urea biosensor. The fit quality is very high, with an R^2 value of 0.98, meaning that 98% of the variation in conductivity is explained by the linear regression [19]. When considering steady-state conductivity, a strong linear correlation is observed between the experimental [14] and theoretical conductivity as a function of urea concentration, as depicted in Figure 6. The Root-Mean-Square Error (RMSE) ≈ 6.5 indicates that the dispersion of the data points around the regression line is relatively low. The derived equation accurately predicts conductivity as a function of urea concentration, providing a solid basis for evaluating the biosensor's key performance characteristics.

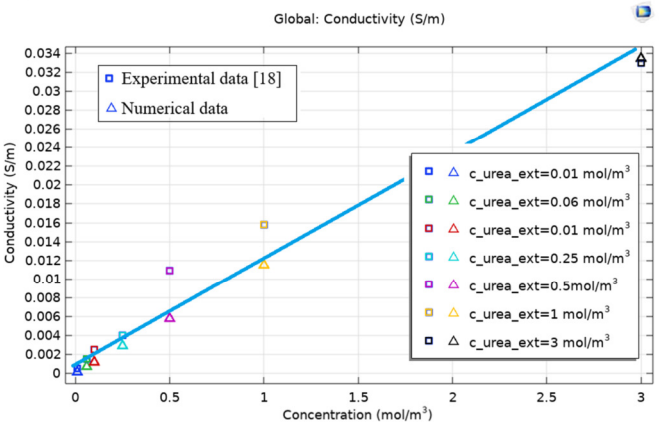

Fig. 6. Experimental [14] and numerical calibration curves of the conductometric urea biosensor.

A metric that plays a crucial role in assessing the performance of conductometric biosensors is sensitivity, defined as the slope of the calibration curve. In this case, it indicates the change in electrical conductivity per unit variation in urea concentration, thus reflecting the biosensor's capability to detect minor fluctuations in the analyte concentration. The sensitivity was calculated at 0.05 S/cm·mM.

C. Influence of Michaelis-Menten Parameters V_{max} and K_M on Sensor Response

The enzymatic activity of the biosensor can be described using the Michaelis-Menten model, which characterizes the kinetics of the urease-catalyzed reaction. Two key parameters in this model are V_{max} and K_M. V_{max} represents the maximum reaction rate achieved when the enzyme is saturated with the substrate, indicating the enzyme's catalytic efficiency under optimal conditions. K_M , the Michaelis-Menten constant, corresponds to the urea concentration at which the reaction rate reaches half of V_{max}. It reflects the enzyme's affinity for urea; a lower K_M value indicates a higher affinity. The following section explores how variations in V_{max} and K_M affect the biosensor's behavior.

A higher V_{max} leads to a greater sensitivity, as it accelerates the enzymatic reaction, increasing the production of ionic species responsible for conductivity. This also reduces the time required to reach reaction saturation, enhancing the sensor's response speed. In contrast, K_M reflects the enzyme's intrinsic affinity for urea. A low K_M value corresponds to higher sensitivity, as the enzyme efficiently catalyzes urea hydrolysis even at low concentrations, resulting in a stronger conductivity response. Conversely, a high K_M leads to a slower and weaker conductivity change, indicating lower sensitivity. While V_{max} can be modulated by adjusting enzyme concentration or temperature (within limits to prevent denaturation), K_M is an intrinsic property of the enzyme and cannot be altered as easily. Therefore, optimizing both parameters is crucial for achieving a fast, sensitive, and stable sensor response.

Figures 7 and 8 demonstrate how varying K_M and V_{max} values affect the conductometric response of the biosensor, respectively.

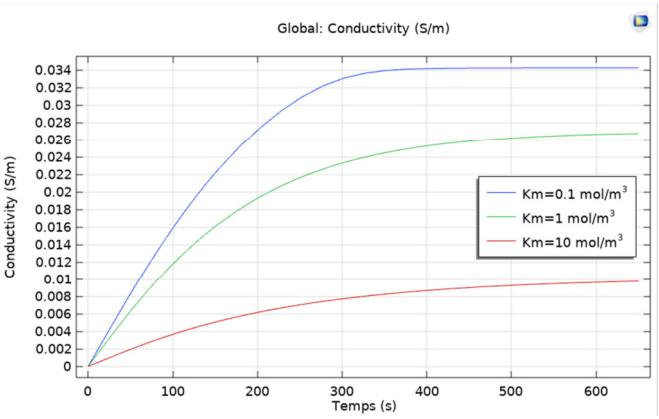

Fig. 7. The effect of K_M on the conductometric response of the biosensor.

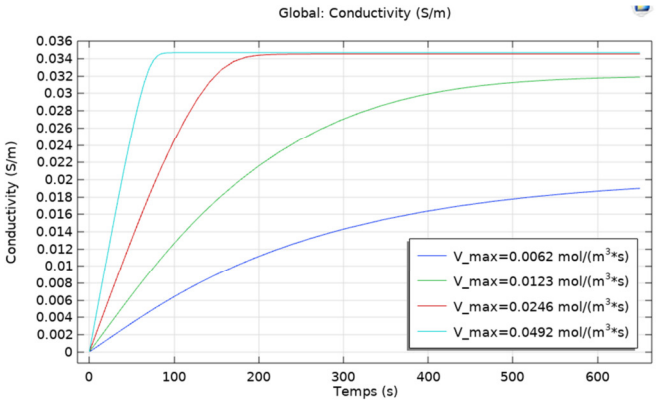

Fig. 8. The effect of V_{max} on the conductometric response of the biosensor.

D. Influence of Temperature on Sensor Response

Temperature also plays a crucial role in the performance of the conductometric urea sensor, as it affects both enzyme activity and ionic mobility. An increase in temperature initially enhances the reaction rate, leading to a higher production of conductive ions (NH_4^+ and OH^-), which improves the sensor's sensitivity. However, beyond an optimal temperature range (35–40°C) [20], the enzyme begins to denature, causing a decline in catalytic efficiency and, consequently, a decrease in conductivity. Additionally, temperature variations influence diffusion rates and ionic mobility, further impacting the sensor's response. Therefore, maintaining an optimal temperature is essential for ensuring accurate and stable measurements.

Figure 9 displays the variation in conductivity (S/m) over time (s) for different temperatures (0°C to 60°C).

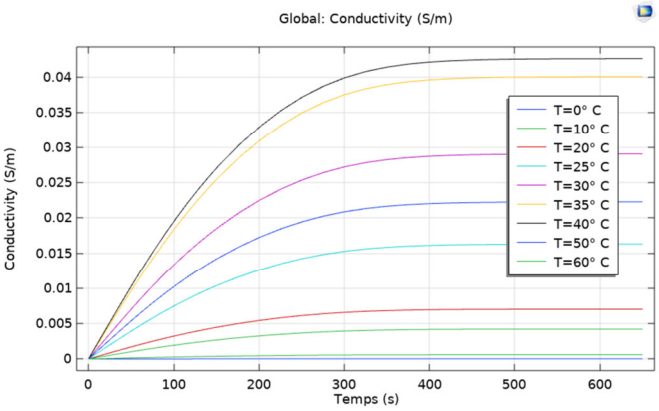

Fig. 9. The effect of temperature on the conductometric response of the biosensor.

As the temperature increases from 0 °C to 40 °C, conductivity rises more rapidly and reaches a higher steady-state value, reflecting an acceleration of the enzymatic reaction and an increased production of ionic species. The optimal temperature range is approximately 35–40 °C, with the highest conductivity being observed around 40 °C, suggesting that this is the most favorable condition for enzymatic activity and

maximum sensor sensitivity. Beyond 40 °C, conductivity reaches a significantly lower peak due to enzyme denaturation, which diminishes the catalytic efficiency of urea hydrolysis and leads to reduced ionic production. The optimal temperature was determined to be 37 °C.

E. Influence of pH and Enzyme Layer Thickness on Sensor Response

Understanding the influence of pH is essential for optimizing biosensor performance, ensuring consistent and accurate measurements, and extending the operational lifespan of the sensor. Variations in pH not only affect the enzymatic activity of urease, but also influence the ionization state of the reaction products, directly impacting the sensor's conductivity response. Additionally, the enzyme layer plays a critical role in modulating the biosensor's behavior under different pH conditions.

Figure 10 presents the response of a conductimetric sensor over time for different pH values. It is observed that conductivity increases over time for all pH values, but at different rates. The highest conductivity values are observed for neutral to slightly acidic pH levels (around pH 7 and pH 8) [20], while lower conductivities are recorded at acidic (pH 4 and 5) and more alkaline (pH 9 and 10) conditions. This behavior indicates that the sensor's response is strongly pH-dependent, with the maximum sensitivity being achieved under near-neutral conditions. At higher pH levels, the production or stability of conductive ions appears reduced, resulting in a less pronounced increase in conductivity. Conversely, under neutral or slightly acidic conditions, ion production is optimized, leading to higher conductivity values and improved sensor performance. The optimal pH level was determined to be 7.4.

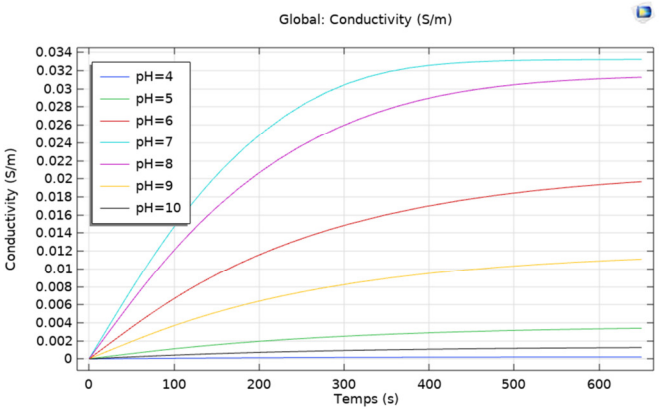

Fig. 10. The effect of the pH on the conductometric response of the biosensor.

Figure 11 depicts the variation of conductivity over time for different enzyme layer thicknesses (L = 1 µm, 10 µm, 100 µm, and 500 µm). Conductivity increases with enzyme layer thickness up to a certain limit. A thicker enzyme layer (L = 100 µm and 500 µm) results in higher conductivity, indicating a greater enzymatic reaction and, consequently, a higher production of ionic species (NH_4^+ and OH^-) that enhance conductivity. However, beyond a certain thickness, a saturation effect is observed: the 100 µm and 500 µm layers reach similar equilibrium conductivity values, suggesting that mass transfer limitations rather than enzymatic activity become the controlling factor. Thin enzyme layers (1 µm and 10 µm) result in lower conductivity. In contrast, thinner enzyme layers (1 µm and 10 µm) yield significantly lower conductivity due to insufficient enzyme quantity, resulting in a reduced conversion of urea into ions. Therefore, while increasing the enzyme layer thickness initially improves performance, beyond a critical threshold, further increases provide no significant benefit.

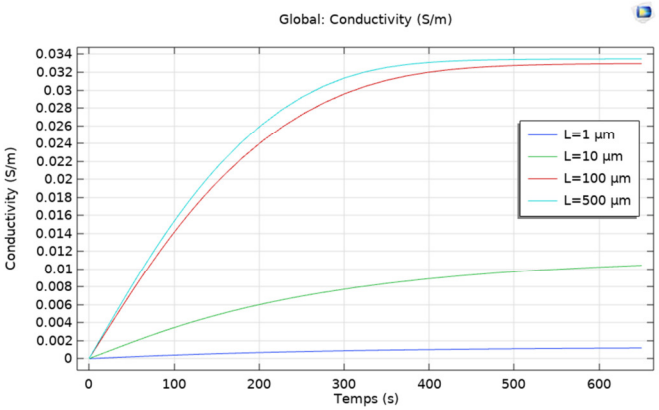

Fig. 11. Variation of conductivity (S/m) over time (s) for different enzyme layer thicknesses.

F. Influence of CO_2 on Sensor Response

During urea hydrolysis, CO_2 is produced and subsequently dissolves in the solution, forming carbonic acid, which can lower the local pH and influence the enzyme activity. This shift in pH affects the ionization of reaction products and, consequently, the conductivity response of the sensor. Thus, CO_2 can play a significant role in the performance of urease-based conductometric biosensors.

Figure 12 illustrates the effect of CO_2 presence or absence on the conductivity response over time during the enzymatic hydrolysis of urea. The curve without CO_2 shows a significantly higher conductivity response compared to the curve with CO_2. This suggests that in the absence of CO_2, urea hydrolysis leads to a greater accumulation of ionic species (NH_4^+ and OH^-), resulting in increased conductivity. When CO_2 is present, the conductivity increase is much lower. This can be attributed to the formation of carbonic acid (H_2CO_3) in solution, which dissociates into bicarbonate (HCO_3^-) and hydrogen ions (H+). The presence of H+ ions shifts the equilibrium of urea hydrolysis, potentially reducing the availability of free NH_3 and OH^-, which are key contributors to conductivity.

In both cases, conductivity initially increases with time, reflecting the progressive hydrolysis of urea. However, without CO_2, conductivity reaches a much higher steady-state value, indicating that the reaction proceeds more efficiently in an alkaline medium. With CO_2, the lower final conductivity suggests that the buffering effect of carbonic acid reduces the impact of urea hydrolysis on the overall ionic concentration. The optimal CO_2 concentration was determined to be 5%.

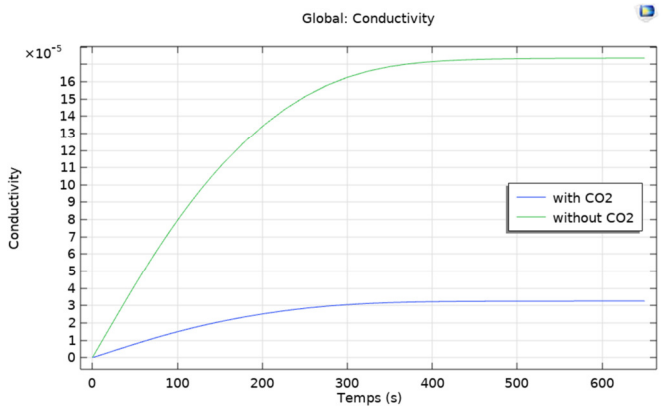

Fig. 12. Effect of CO_2 presence or absence on the conductivity response over time.

V. CONCLUSION

In this study, a mathematical model predicting the response of a conductometric urea biosensor was developed and validated through experimental results. The model, implemented using COMSOL Multiphysics, accurately simulated the key physicochemical processes affecting the biosensor's performance, including the effects of temperature, pH, enzyme layer thickness, and CO_2 concentration. The validation of the model against experimental data demonstrated strong agreement, confirming its reliability in predicting the sensor's behavior. Temperature was found to significantly influence the enzymatic activity of urease, with the optimal response being observed at 37°C, reflecting the enzyme's maximum catalytic efficiency at physiological conditions. Similarly, pH variations affected the ionization state of both the enzyme and the reaction products, with optimal conductivity changes being recorded at pH 7.4, aligning with the urease activity peak. The enzyme layer thickness also played a crucial role, as it influenced the diffusion of urea and the generated ionic products. Simulations indicated that an enzymatic layer thickness of 500 µm provided the best balance between reaction efficiency and diffusion limitations. Additionally, the presence of CO_2 was shown to impact the local pH due to the formation of carbonic acid, with a concentration of 5% CO_2 yielding the most stable and optimal sensor response.

Overall, the numerical simulations provided valuable insights into the interplay of these parameters, supporting the design and optimization of the biosensor for practical applications. The close match between the simulated and experimental results underscores the potential of COMSOL-based modeling as a powerful tool in biosensor development. These findings contribute to the advancement of conductometric urea biosensors, with promising applications in biomedical diagnostics and environmental monitoring.

REFERENCES

[1] N. F. Sheppard, D. J. Mears, and A. Guiseppi-Elie, "Model of an immobilized enzyme conductimetric urea biosensor," *Biosensors and Bioelectronics*, vol. 11, no. 10, pp. 967–979, 1996, https://doi.org/10.1016/0956-5663(96)87656-1.

[2] Valdes, J. J., Wall Jr, J. G., Chambers, J. P., and Eldefrawi, M. E. "A receptor-based capacitive biosensor," *Johns Hopkins APL Technical Digest*, vol. 9, no. 1, pp. 4-9, 1988.

[3] R. F. Taylor, I. G. Marenchic, and E. J. Cook, "An acetylcholine receptor-based biosensor for the detection of cholinergic agents," *Analytica Chimica Acta*, vol. 213, pp. 131–138, 1988, https://doi.org/10.1016/S0003-2670(00)81347-1.

[4] D. C. Cullen, R. S. Sethi, and C. R. Lowe, "Multi-analyte miniature conductance biosensor," *Analytica Chimica Acta*, vol. 231, pp. 33–40, 1990, https://doi.org/10.1016/S0003-2670(00)86394-1.

[5] S. R. Mikkelsen and G. A. Rechnitz, "Conductometric tranducers for enzyme-based biosensors," Analytical Chemistry, vol. 61, no. 15, pp. 1737–1742, Aug. 1989, https://doi.org/10.1021/ac00190a029.

[6] M. Singh, N. Verma, A. Garg, and N. Redhu, "Urea biosensors," *Sensors and Actuators B: Chemical*, vol. 134, no. 1, pp. 345–351, Aug. 2008, https://doi.org/10.1016/j.snb.2008.04.025.

[7] C.-Y. Lai, P. Foot, J. Brown, and P. Spearman, "A Urea Potentiometric Biosensor Based on a Thiophene Copolymer," *Biosensors*, vol. 7, no. 1, Mar. 2017, Art. no. 13, https://doi.org/10.3390/bios7010013.

[8] K. Sihombing, M. C. Tamba, W. S. Marbun, and M. Situmorang, "Urease immobilized potentiometric biosensor for determination of urea," *Indian Journal of Chemistry - Section A Inorganic, Physical, Theoretical and Analytical Chemistry*, vol. 57A, pp. 175–180, Feb. 2018.

[9] S. Bekkouche and M. Kadja, "Numerical Analysis of Density-Driven Reactive Flows in Hele-Shaw Cell Geometry," *Engineering, Technology & Applied Science Research*, vol. 10, no. 2, pp. 5434–5440, Apr. 2020, https://doi.org/10.48084/etasr.3349.

[10] B. Sahin and T. Kaya, "Electrochemical amperometric biosensor applications of nanostructured metal oxides: a review," *Materials Research Express*, vol. 6, no. 4, Jan. 2019, Art. no. 042003, https://doi.org/10.1088/2053-1591/aafa95.

[11] S. K. Kirdeciler *et al.*, "A novel urea conductometric biosensor based on zeolite immobilized urease," *Talanta*, vol. 85, no. 3, pp. 1435–1441, Sep. 2011, https://doi.org/10.1016/j.talanta.2011.06.034.

[12] *COMSOL Multiphysics.* (Version 5.6), COMSOL Inc. [Online]. Available: https://www.comsol.com

[13] T. P. Velychko *et al.*, "A Novel Conductometric Urea Biosensor with Improved Analytical Characteristic Based on Recombinant Urease Adsorbed on Nanoparticle of Silicalite," *Nanoscale Research Letters*, vol. 11, no. 1, Dec. 2016, Art. no. 106, https://doi.org/10.1186/s11671-016-1310-3.

[14] F. Zouaoui, N. Zine, A. Errachid, and N. Jaffrezic-Renault, "Mathematical Model and Numerical Simulation of Conductometric Biosensor of Urea," *Electroanalysis*, vol. 34, no. 7, pp. 1131–1140, Jul. 2022, https://doi.org/10.1002/elan.202100610.

[15] S. R. Eisenberg and A. J. Grodzinsky, "The Kinetics of Chemically Induced Nonequilibrium Swelling of Articular Cartilage and Corneal Stroma," *Journal of Biomechanical Engineering*, vol. 109, no. 1, pp. 79–89, Feb. 1987, https://doi.org/10.1115/1.3138647.

[16] K. B. Ramachandran and D. D. Perlmutter, "Effects of immobilization on the kinetics of enzyme-catalyzed reactions. II. Urease in a packed-column differential reactor system," *Biotechnology and Bioengineering*, vol. 18, no. 5, pp. 685–699, May 1976, https://doi.org/10.1002/bit.260180508.

[17] J. K. Leypoldt and D. A. Gough, "Model of a two-substrate enzyme electrode for glucose," *Analytical Chemistry*, vol. 56, no. 14, pp. 2896–2904, Dec. 1984, https://doi.org/10.1021/ac00278a063.

[18] M. C. Zaretsky, L. Mouayad, and J. R. Melcher, "Continuum properties from interdigital electrode dielectrometry," *IEEE Transactions on Electrical Insulation*, vol. 23, no. 6, pp. 897–917, Dec. 1988, https://doi.org/10.1109/14.16515.

[19] H. Waheed and A. Hussain, "Effect of Polyvinyl Pyrolidone on Morphology and Performance of Cellulose Acetate Based Dialysis Membrane," *Engineering, Technology & Applied Science Research*, vol. 9, no. 1, pp. 3744–3749, Feb. 2019, https://doi.org/10.48084/etasr.2491.

[20] D. L. Filmer and T. G. Cooper, "Effect of varying temperature and pH upon the predicted rate of 'CO2' utilization by car□ylases," *Journal of Theoretical Biology*, vol. 29, no. 1, pp. 131–145, Oct. 1970, https://doi.org/10.1016/0022-5193(70)90122-0.